



# Geophysical Research Letters

## RESEARCH LETTER

10.1029/2019GL082140

### Key Points:

- We provide the first statistical study to comprehensively describe this mysterious power gap of chorus waves in the Earth's magnetosphere
- Overall, there are about 2/3 of events identified to have a power gap between two bands, and 1/3 of events are observed without a power gap
- We have studied the distribution of both the gap frequency and frequency width of the power gap and their dependencies on two bands

### Supporting Information:

- Supporting Information S1
- Figure S1
- Figure S2

### Correspondence to:

Q. Lu,  
qmlu@ustc.edu.cn

### Citation:

Gao, X., Chen, L., Li, W., Lu, Q., & Wang, S. (2019). Statistical results of the power gap between lower-band and upper-band chorus waves. *Geophysical Research Letters*, 46, 4098–4105. <https://doi.org/10.1029/2019GL082140>

Received 20 JAN 2019

Accepted 31 MAR 2019

Accepted article online 10 APR 2019

Published online 23 APR 2019

©2019. American Geophysical Union.  
All Rights Reserved.

## Statistical Results of the Power Gap Between Lower-Band and Upper-Band Chorus Waves

Xinliang Gao<sup>1,2</sup>, Lunjin Chen<sup>3</sup>, Wen Li<sup>4</sup>, Quanming Lu<sup>1,2</sup>, and Shui Wang<sup>1,2</sup>

<sup>1</sup>CAS Key Laboratory of Geospace Environment, Department of Geophysics and Planetary Science, University of Science and Technology of China, Hefei, China, <sup>2</sup>Collaborative Innovation Center of Astronautical Science and Technology, Harbin, China, <sup>3</sup>Department of Physics, University of Texas at Dallas, Richardson, TX, USA, <sup>4</sup>Center for Space Physics, Boston University, Boston, MA, USA

**Abstract** The primary power gap of chorus waves is statistically investigated using 7-year waveform data from THEMIS probes for the first time. Overall, ~2/3 of chorus events have a power gap between the lower and upper bands. Both the gap frequency and the frequency bandwidth of the gap have a broad distribution, which peaks at frequencies of  $\sim 0.49f_{ce}$  and  $\sim 0.07f_{ce}$ , respectively. The gap frequency tends to increase with increasing  $|MLAT|$  (magnetic latitude), while the frequency width gradually increases with  $L$ -shell. In most of banded events, the peak frequency of upper band is roughly twice that of lower band. Two types of events are studied. For Type I events, one population is located around  $P_{up}/P_{low} = 10^{-1}$ , and the other is around  $P_{up}/P_{low} = 10^{-3}$ . However, Type II events are roughly concentrated around  $P_{up}/P_{low} = 10^{-3}$ . The gap frequency positively correlates with the frequency of upper band. Our study provides detailed observational constraints on potential mechanisms of the power gap formation.

### 1. Introduction

Whistler-mode chorus wave in the Earth's magnetosphere has received great attention over the past several decades not only because of its dual role in both accelerating and scattering energetic electrons (Ni et al., 2011; Reeves et al., 2013; Thorne et al., 2010, 2013; Xiao et al., 2014) but also because of its unique observational properties (Burtis & Helliwell, 1969; Li et al., 2012). One of them is the power gap around  $0.5f_{ce}$  (where  $f_{ce}$  is the equatorial electron gyrofrequency) in the time-frequency spectrogram, which divides chorus waves into two bands: lower band ( $0.1\text{--}0.5f_{ce}$ ) and upper band ( $0.5\text{--}1.0f_{ce}$ ; Meredith et al., 2001; Tsurutani & Smith, 1974). Very few studies aim to understand this banded spectral structure, which has been a longstanding problem in magnetospheric physics. According to the nonlinear wave growth theory, Omura et al. (2009) proposed that chorus waves can be excited over a continuous spectrum from the lower to upper bands, but they may experience a strong damping around  $0.5f_{ce}$  during their propagation (Hsieh & Omura, 2018; Tsurutani & Smith, 1974). This mechanism was further supported by the analysis of both lower-band and upper-band chorus waves recorded by Geotail satellites in the outer magnetosphere ( $L > 9$ ; Habagishi et al., 2014; Yagitani et al., 2014). Another damping effect caused by subcyclotron resonances was also proposed to explain the power gaps (Fu et al., 2015). A banded chorus event detected by Van Allen Probes (Fu et al., 2014), on the other hand, implies that the power gap is a natural consequence of two bands excited by two distinct electron populations. Recently, Gao et al. (2016, 2017), Gao, Lu, and Wang (2018), and Gao, Lu, Wang, et al. (2018) have done a series of studies about multiband chorus waves in the Earth's magnetosphere, where upper-band waves are excited through the coupling between electromagnetic and electrostatic components of lower-band waves (i.e., lower band cascade), and as a result a power gap is formed. Due to the high occurrence of multiband chorus waves [Gao, Lu, Wang, et al., 2018], they pointed out that the lower-band cascade could be a significant potential mechanism to generate the banded spectrum. To fully understand the power gap, a comprehensive statistical study on its properties is quite urgent and valuable. In this letter, we investigate the power gap between lower-band and upper-band chorus waves by using long-term THEMIS waveform data, including the distribution of both the gap frequency and frequency bandwidth of the power gap and their dependencies on two bands. So far, this is the first statistical study to specifically investigate the gap frequency and frequency bandwidth of the power gap.

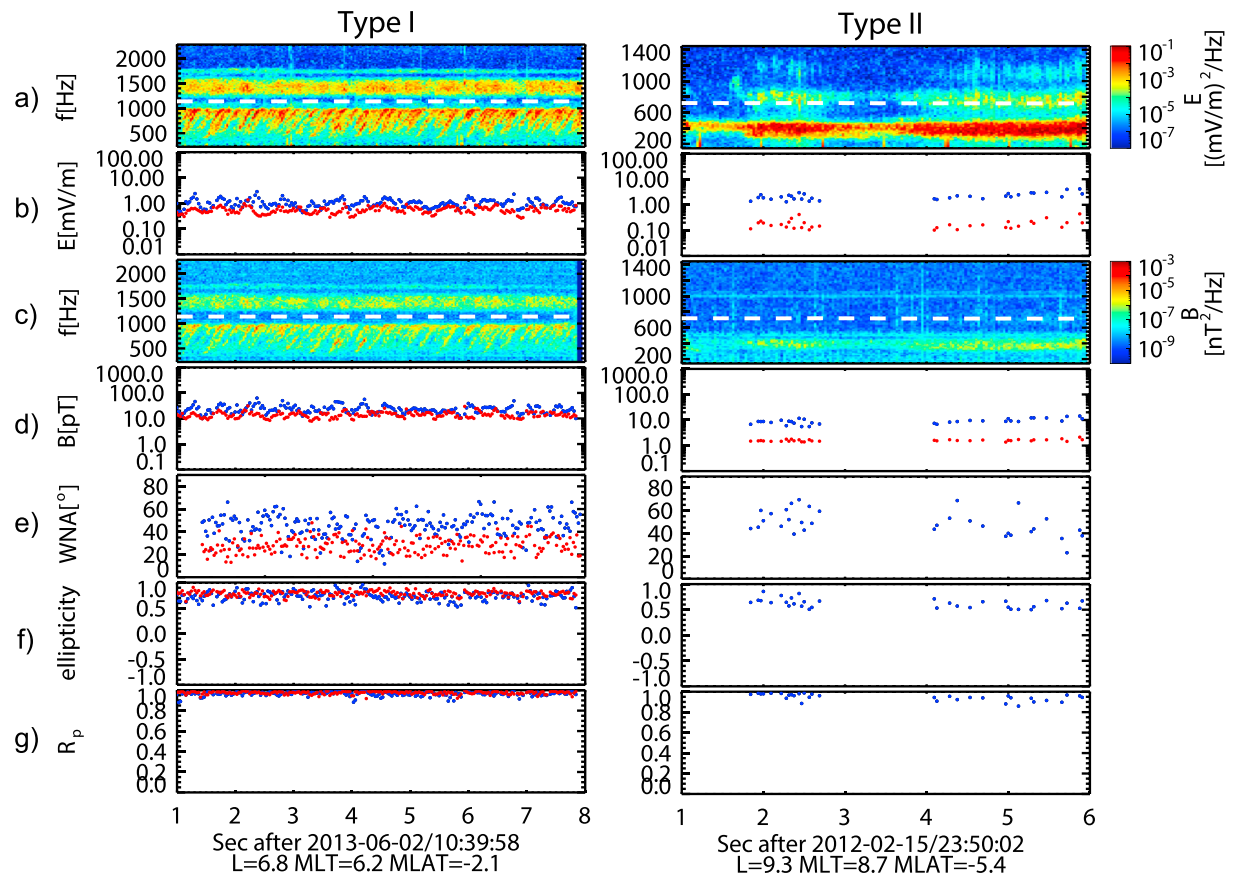


**Figure 1.** (a) The electric spectrogram, (b) electric amplitude, (c) magnetic spectrogram, (d) magnetic amplitude, (e) wave normal angle, (f) ellipticity, and (g) polarization ratio ( $R_p$ ) for two types of chorus waves containing both lower and upper bands. The white dashed line in Figure 1a represents  $0.5f_{ce}$ . The red and blue dots represent wave parameters at each selected time for upper and lower band, respectively.

## 2. THEMIS Data Analysis

The power gap of chorus waves is analyzed using the waveform data collected from search coil magnetometer (Roux et al., 2008) and Electric Field Instrument (Bonnell et al., 2008) onboard three inner THEMIS (Time History of Events and Macroscale Interactions During Substorms) probes (A, D, and E; Angelopoulos, 2008) during the period from June 2008 to June 2015. The sampling frequency of waveform bursts is  $\sim 8$  kHz, and each one lasts about 6–8 s. For each waveform data, we conduct a 512-point fast Fourier transform with a 256-point sliding window to obtain the magnetic and electric spectrograms with a time resolution of  $\sim 0.032$  s. To obtain detailed wave polarization properties (such as ellipticity and polarization ratio), all data have been routinely processed in the field-aligned coordinated system following the procedure developed by Bortnik et al. (2007).

Figure 1 is an overview plot showing two different types of chorus waves containing both lower and upper bands, including (a) the electric spectrogram, (b) electric amplitude, (c) magnetic spectrogram, (d) magnetic amplitude, (e) wave normal angle, (f) ellipticity, and (g) polarization ratio ( $R_p$ ). For Type I event, upper bands are found in both electric and magnetic spectrograms (left column of Figures 1a and 1c). In contrast, Type II event has the upper-band waves that are only detected in the electric spectrogram (right column of Figures 1a and 1c). At each time, we calculate the root-mean-square magnetic (electric) amplitude by integrating the magnetic (electric) power over  $0.1-0.5f_{ce}$  and  $0.5-1f_{ce}$  for lower band and upper band, respectively. Meanwhile, we obtain the average ellipticity and  $R_p$  weighted by the magnetic power for Type I event or the electric power for Type II event over each of the two bands. We use the following criteria to identify Types I and II: for Type I event,  $R_p$  of each band  $> 0.7$ , ellipticity of each band  $> 0.5$ , magnetic amplitude of lower band  $> 5$  pT, and magnetic amplitude of upper band  $> 2$  pT; for Type II event,  $R_p$  of lower band  $> 0.7$ ,

ellipticity of lower band  $>0.5$ , magnetic amplitude of lower band  $>5$  pT, magnetic amplitude of upper band  $<2$  pT, and electric amplitude of upper band  $>0.1$  mV/m. Note that Figure 1 only exhibits those data points (red or blue dots) satisfying the above criteria for the two examples. Finally, there must be at least 10 data points (i.e.,  $\sim 0.3$  s) over the entire chorus waveform duration (6–8 s). Since the measurement of magnetic fields is subject to less contamination than that of electric fields for THEMIS probes, we preferentially use magnetic fields to check if each waveform data satisfies the above criteria of Type I event. If not, we further check this data segment by analyzing electric fields.

Using the criteria described above, we have constructed an extensive data set (1837 samples for Type I and 616 samples for Type II; each sample is a 6–8 s waveform event) of chorus events simultaneously containing two bands over the extensive coverage from 4 to 10  $R_E$  in all magnetic local time (MLT) sectors. It is worth nothing that this chorus wave data set includes emissions with rising tones, falling tones, and hiss-like emissions, and we do not distinguish their specific types in the present study, since the banded structure is more like a common feature among different types of chorus waves in the Earth's magnetosphere. Besides, most of Type II events have very large wave normal angles.

### 3. Statistical Results

In this study, we use two parameters, the gap frequency  $f_{gap}$  and frequency bandwidth  $f_{width}$  of the power gap, to describe the power gap, as shown in Figures 2a and 2b. Figures 2a and 2b present the power distribution in the frequency for the two examples in Figure 1, which is obtained by averaging all selected time points in each event. We first identify the power peak in each band, which is marked by blue (lower band) or red (upper band) dot in the two panels. It is worth noting, however, that if there are more than one clear power peaks in one band, then we only record the peak closest to  $0.5 f_{ce}$ . In other words, we only focused on the primary gap near  $0.5 f_{ce}$  in the power spectrum of chorus waves. The gap frequency of the power gap is then defined as the frequency of the power minimum between the two bands, which is denoted by the purple dot in Figures 2a and 2b. The blue line in each panel marks one fifth of the smaller value of two power peaks ( $P_{th1}$ ), while the red line marks the power threshold ( $P_{th2}$ ) of  $6.25 \times 10^{-8}$  nT<sup>2</sup>/Hz (Type I event) or  $1.6 \times 10^{-4}$  (mV/m)<sup>2</sup>/Hz (Type II event). We identify a chorus event as a banded one with a power gap only if the power minimum is smaller than both  $P_{th1}$  and  $P_{th2}$ . The frequency bandwidth of the power gap, if identified, is given by the width of the frequency range with the power below the smaller value between  $P_{th1}$  and  $P_{th2}$ .

Figures 2c and 2d present the distribution of all selected chorus events regardless of the power gap in the ( $R_{gap}, P_{gap}$ ) plane for Types I and II, respectively. Here  $P_{gap}$  denotes the power minimum between two bands. The  $R_{gap}$  is the ratio between the  $P_{gap}$  and the smaller one of two power peaks (Figures 2a or 2b). In each panel, the black and magenta dashed lines mark the value of 0.2 and  $P_{th2}$ , respectively. Again, we require banded chorus events (with a power gap) to satisfy  $P_{gap} < P_{th2}$  and  $R_{gap} < 0.2$ . About two thirds of all selected chorus events (1323 for Type I and 392 for Type II) identified have a power gap between two bands, which will be further analyzed in the following part. Surprisingly, there are also many chorus events in our data set (about one third) without a power gap, in which either the power minimum is too strong ( $P_{gap} > P_{th2}$ ) or the gap is too shallow ( $R_{gap} > 0.2$ ).

The distributions of the gap frequency ( $f_{gap}/f_{ce}$ ) and width ( $f_{width}/f_{ce}$ ) of the power gap are illustrated in Figures 3a and 3b for both Types I (blue) and II (red) banded chorus events. Here the percentage is given by the ratio between the event number in each bin to the total number of banded chorus events. The distribution of the gap frequency  $f_{gap}/f_{ce}$  indeed peaks at the frequency around  $0.49 f_{ce}$  (the corresponding frequency bin of  $0.48$ – $0.5 f_{ce}$  with the percentage of  $\sim 28\%$ ), but it can vary over a broad frequency range of  $0.36$ – $0.7 f_{ce}$ . We have illustrated two banded chorus events in the supporting information, whose gap frequencies are at the boundary of the distribution. Besides, the distribution of  $f_{gap}/f_{ce}$  is clearly asymmetric about  $0.5 f_{ce}$ , with more banded chorus events of a power gap below  $0.5 f_{ce}$ . As shown in Figure 4b, the frequency width of power gap  $f_{width}/f_{ce}$  also has a broad distribution in frequency (from 0 to  $0.3 f_{ce}$ ), peaking at about  $0.07 f_{ce}$  (the frequency bin of  $0.06$ – $0.08 f_{ce}$  with the percentage of  $\sim 16\%$ ). Figure 3c is a scatterplot in the ( $f_{gap}, f_{width}$ ) plane, where each dot represents one banded chorus event and the median  $f_{width}/f_{ce}$  is denoted by the cyan line with the first and third quartiles shown in vertical cyan bars. In

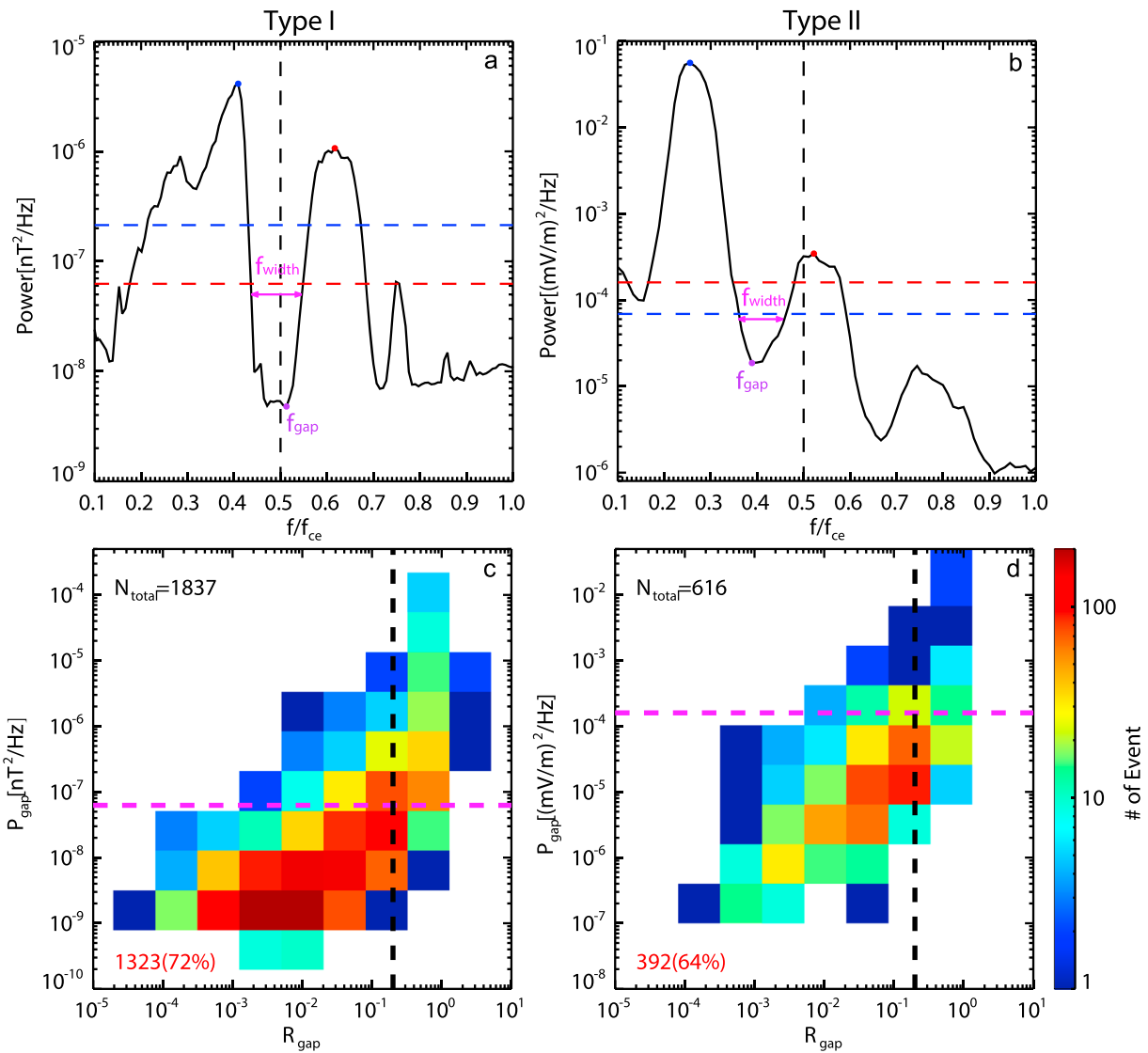


**Figure 2.** (a, b) The power distribution in the frequency for two examples in Figure 1. Blue and red dots denote the selected power peak in lower band and upper band, respectively. The position of the power minimum between two bands is marked by the purple dot. The blue line in each panel marks one fifth of the smaller one of two power peaks ( $P_{th1}$ ), whereas the red line marks the power threshold ( $P_{th2}$ ) of  $6.25 \times 10^{-8} nT^2/Hz$  (panel a) or  $1.6 \times 10^{-4} (mV/m)^2/Hz$  (panel b). (c, d) The distribution of all selected chorus events in the ( $R_{gap}, P_{gap}$ ) plane for Types I and II, respectively. The  $R_{gap}$  is the ratio between the  $P_{gap}$  and the smaller one of two power peaks. In each panel, the black and magenta dashed lines mark the value of 0.2 and  $P_{th2}$ , respectively.

Figure 3c, there is only a weak trend that the width of power gap is narrower when its gap frequency is closer to the frequency of  $0.5 f_{ce}$ .

The global distribution of banded chorus events is exhibited in Figures 3d–3f, where the percentage (left y axis) is defined by the ratio of the number of samples in each bin to the total number of samples. The magenta line in each panel represents the median  $f_{gap}/f_{ce}$  (right y axis) in the bin of at least five samples, with the first and third quartiles shown in vertical bars. The cyan line represents the result of  $f_{width}/f_{ce}$  (right y axis) in the same format. Similar to the distribution of lower-band chorus waves shown in Li et al. (2012), banded chorus waves also preferentially occur at larger  $L$ -shells ( $L > 6$ ; may be partially due to more THEMIS waveform data captured at larger  $L$ -shells (Gao, Lu, Wang, et al., 2018)), in dawn and morning sectors ( $4 \text{ hr} < \text{MLT} < 10 \text{ hr}$ ), and in equatorial regions ( $|\text{MLAT}| < 10^\circ$ ). Moreover, we further find that the gap frequency of the power gap is nearly independent on the  $L$ -shell (Figure 3d) and MLT (Figure 3e), but the power gap tends to shift to higher frequencies with increasing  $|\text{MLAT}|$  (Figure 3f). Meanwhile, the

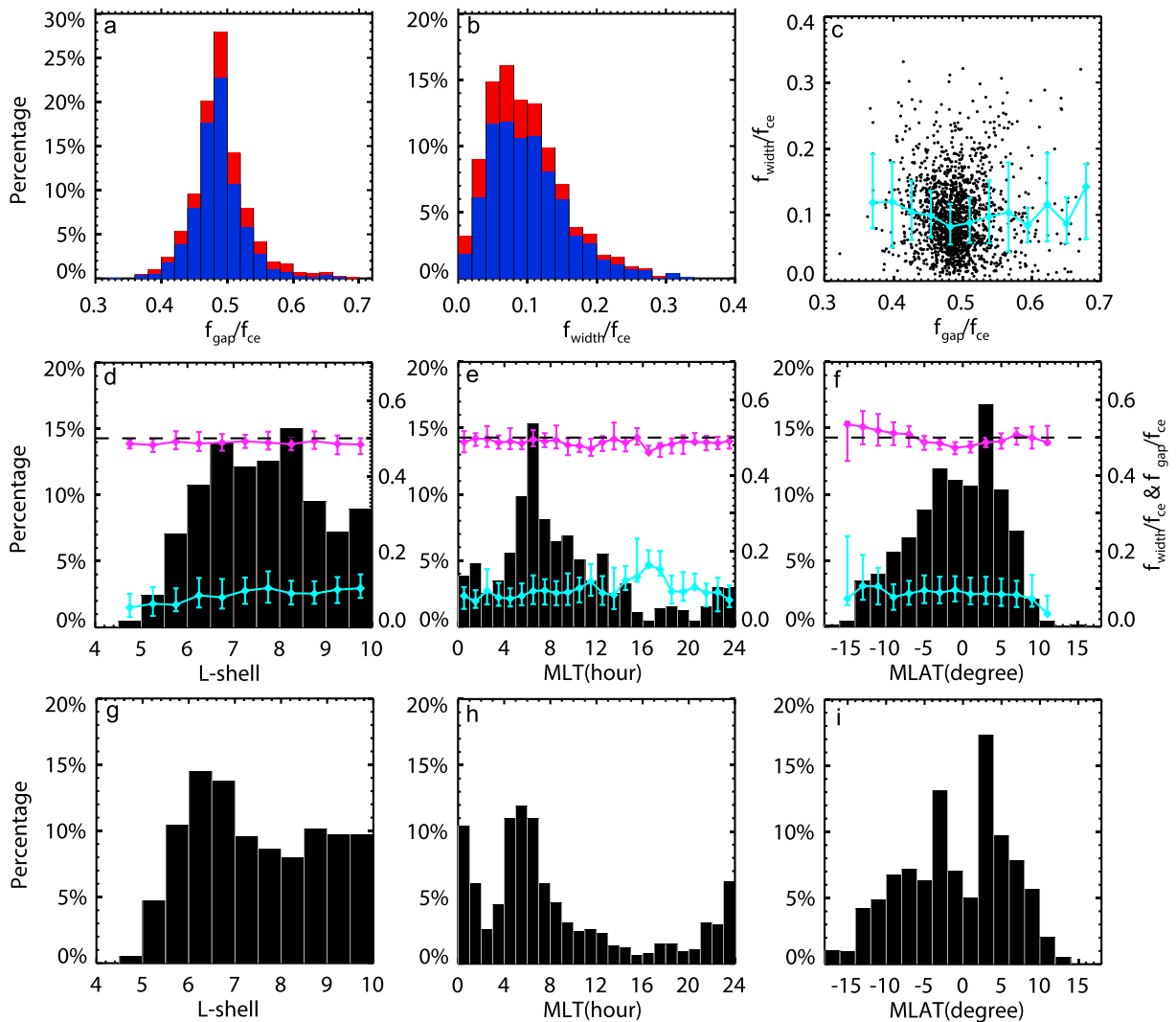


**Figure 3.** The distribution of (a) the gap frequency ( $f_{gap}/f_{ce}$ ) and (b) frequency width ( $f_{width}/f_{ce}$ ) for both Types I (blue) and II (red) banded chorus events. (c) The scatterplot of samples in the ( $f_{gap}$ ,  $f_{width}$ ) plane. The median  $f_{width}/f_{ce}$  is denoted by the cyan line with the first and third quartiles shown in vertical cyan bars. The global distribution of banded events versus (d)  $L$ -shell, (e) MLT, and (f) MLAT, respectively. The magenta line in each panel represents the median  $f_{gap}/f_{ce}$  (right y axis) in the bin with the first and third quartiles shown in vertical bars. The cyan line gives the result of  $f_{width}/f_{ce}$  (right y axis) in the same way. The global distribution of chorus events without the gap versus (g)  $L$ -shell, (h) MLT, and (i) MLAT, respectively.

frequency bandwidth of the power gap is observed to be nearly invariant with MLAT (Figure 3f) and tends to have larger values at larger  $L$ -shells. Note that although the width of the power gap somehow becomes much larger in the dusk sector ( $14 \text{ hr} < \text{MLT} < 18 \text{ hr}$ ), its statistical significance may be not high since only few samples are recorded in this sector. We have also shown the global distribution of chorus emissions without the power gap in Figures 3g–3i. Their distribution is quite similar to that of banded chorus events. A noticeable exception, however, is that there is a relatively lower percentage at the magnetic equator for chorus events without the power gap (Figure 3i).

We have further investigated the dependences of the power gap on both lower-band and upper-band chorus waves. Figure 4a presents the distribution of event number in the ( $f_{low}f_{up}$ ) plane for all banded events. The distribution of event number for Type I and II events in the ( $P_{low}P_{up}$ ) plane is shown in Figures 4b and 4c, respectively. The  $P_{low}$  and  $P_{up}$  are power peaks in lower and upper bands, respectively, while the  $f_{low}$  and  $f_{up}$  are the frequencies of power peaks in lower and upper bands, respectively. In Figure 4a, it is interesting to find that banded chorus events are concentrated around the magenta line ( $f_{up}/f_{low} = 2$ ), suggesting that the frequency of upper-band power peak is roughly two times that of

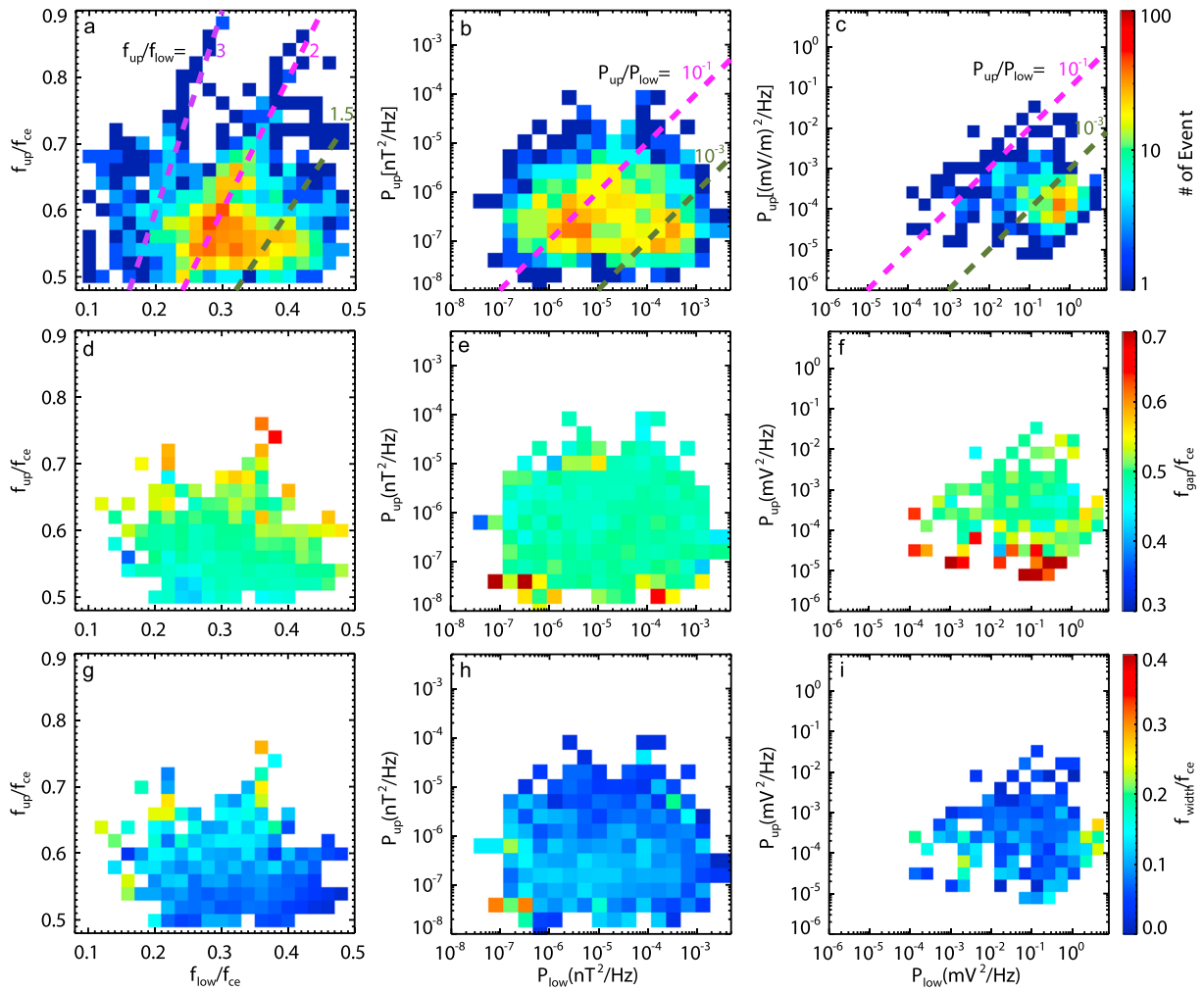


**Figure 4.** The distribution of event number (a) in the  $(f_{low}, f_{up})$  plane for all banded events, and in the  $(P_{low}, P_{up})$  plane for Type (b) I and (c) II events, respectively. In panel a, the olive, magenta, and purple lines denote  $f_{up}/f_{low} = 1.5, 2,$  and  $3,$  respectively. In panels b and c, the magenta and olive lines represent  $P_{up}/P_{low} = 10^{-1}$  and  $10^{-3},$  respectively. The distribution of (d, e, and f) the gap frequency and (g, h, and i) frequency width of the power gap in the same format as top row.

lower band. Besides, there is also a significant population around the olive line ( $f_{up}/f_{low} = 1.5$ ), and a minor population along the purple line ( $f_{up}/f_{low} = 3$ ). For Type I events, two distinct populations can be observed in the  $(P_{low}, P_{up})$  plane (Figure 4b). One is around the magenta line ( $P_{up}/P_{low} = 10^{-1}$ ), meaning the magnetic amplitude of upper-band waves is only several times smaller than that of lower-band waves. The other is around the olive line ( $P_{up}/P_{low} = 10^{-3}$ ), which indicates the magnetic amplitude of upper-band waves is 1–2 orders smaller than that of lower-band waves. However, as shown in Figure 4c, the majority of Type II events are found to have much weaker upper-band waves, whose electric amplitudes are usually 1–2 orders smaller than lower-band chorus waves.

In the same format, Figures 4d–4f (Figures 4g–4i) show the results for the gap frequency (frequency bandwidth) of the power gap. Here, bins with less than 3 samples are discarded. In Figure 4d, it is shown that the gap frequency positively correlates with the frequency of the upper-band waves but does not with the frequency of lower-band waves. As shown in Figures 4e and 4f, some events with very large gap frequencies ( $>0.6f_{ce}$ ) of the power gap are found to have very weak upper bands. As expected, the frequency bandwidth of the power gap is well correlated with the frequency difference between two bands (Figure 4g) rather than their powers (Figures 4h and 4i). We have also studied the dependence of the power gap on wave normal angles in the supporting information. There is a significant population falling within the region where the difference between wave normal angles of two bands is smaller than 10 degree.

#### 4. Summary and Discussion

In this paper, we have statistically investigated the power gap of banded chorus events by analyzing 7-year waveform data from three inner THEMIS probes. So far, this is the first statistical study to specifically evaluate the gap frequency and frequency bandwidth of the power gap of chorus waves in the Earth's magnetosphere. The principal results are summarized as follows:

1. Under our definition, for chorus waves simultaneously containing both bands, there are about two thirds of events identified to have a power gap between two bands, and one third of events are observed without a power gap. Moreover, two types of banded chorus events have been presented: In Type I events, upper band is observed in both electric and magnetic spectrograms, and in Type II events, upper band is only detected in the electric spectrogram.
2. The gap frequency of the power gap has a broad distribution ranging from  $0.36$  to  $0.7 f_{ce}$ , which peaks at the frequency of  $\sim 0.49 f_{ce}$ . The distribution of the frequency bandwidth also covers a wide frequency range (from  $0$  to  $0.3 f_{ce}$ ), peaking at the frequency of  $\sim 0.07 f_{ce}$ . The gap frequency is nearly independent on the  $L$ -shell and MLT, but it tends to shift to higher frequencies with increasing  $|MLAT|$ . Moreover, the frequency bandwidth of the power gap is observed to be nearly invariant with MLAT and MLT but gradually increases with increasing  $L$ -shell.
3. Interestingly, the frequency of upper-band waves is roughly two times that of lower band in most of banded chorus events. For Type I events, two distinct populations can be observed in the  $(P_{low}, P_{up})$  plane: One is around  $P_{up}/P_{low} = 10^{-1}$ , and the other is around  $P_{up}/P_{low} = 10^{-3}$ . The majority of Type II events are found to have much weaker upper-band waves, whose electric amplitudes are usually 1–2 orders smaller than lower-band chorus waves. The gap frequency of the power gap is more correlated with the frequency of upper-band waves than lower-band waves, i.e., the gap frequency is almost uniformly distributed across the lower band frequency, but has a weak linear dependence on the upper band frequency.

The power gap between two bands has long been considered as a unique and well-known property of chorus waves in the Earth's magnetosphere, but its formation mechanism still remains a challenge. Although several potential mechanisms have been proposed, none of them can fully explain the observational properties presented above. Tsurutani and Smith (1974) and Omura et al. (2009) speculated chorus waves may experience a strong damping near  $0.5 f_{ce}$  during the propagation, which then finally causes a power gap between two bands. This mechanism may easily explain why the gap frequency of the power gap is usually observed around  $0.5 f_{ce}$  but cannot well explain the broad distribution of the gap frequency. Moreover, in this scenario, the frequency of upper-band waves is expected to be only a little bit larger than that of lower-band waves, since chorus waves are thought to be consecutively excited from the lower to upper band. Through the lower band cascade proposed by Gao et al. (2016), the upper-band waves tend to be excited at the frequencies around two times that of lower-band waves and then a power gap will be naturally formed somewhere between two bands. Because the lower-band waves cover a wide range of frequencies, the gap frequency and the bandwidth of the power gap will also have a broad distribution in frequency. In this scenario, the amplitude of upper-band waves is usually 1–2 orders smaller than that of lower-band waves, which may well explain most of Type II events and part of Type I events. However, this mechanism seems not working for those banded chorus events where the power of upper-band waves is just slightly smaller than that of lower-band waves. The idea from Fu et al. (2014) implies that the power gap is the consequence of two bands excited by two distinct electron populations, which may result in many possibilities of the gap frequency and bandwidth of the power gap. However, it is quite difficult to explain the correlation between two bands presented in Figure 4. Moreover, the required unrealistic anisotropy of lower-energy electrons to generate upper-band waves still challenges its applicability in the Earth's magnetosphere. Another damping effect through subcyclotron resonances with thermal electrons (Fu et al., 2015) may cause power gaps at several specific frequencies, such as  $1/3$ ,  $1/2$ , and  $2/3$  local electron gyrofrequency. However, this mechanism needs to be further supported by self-consistent simulations and observations. Therefore, we suggest the power gap could be the result of a combination of several different mechanisms. Our statistical results may not only provide some experimental constraints on the existing mechanisms but also require new mechanisms to understand the banded structure of chorus waves.

### Acknowledgments

This work was supported by the NSFC grant numbers 41774151, 41604128, 41631071, and 41474125, Youth Innovation Promotion Association of Chinese Academy of Sciences (grant number 2016395), Young Elite Scientists Sponsorship Program by CAST (2018QNR001), and Key Research Program of Frontier Sciences, CAS (QYZDJ-SSW-DQC010. L. C. acknowledges the support of the AFOSR grant of FA9550-16-1-0344. W. L. would like to acknowledge the Alfred P. Sloan Research Fellowship FG-2018-10936. We also acknowledge the entire THEMIS instrument group and the THEMIS data obtained from <http://themis.ssl.berkeley.edu/data/themis> website.

### References

- Angelopoulos, V. (2008). The THEMIS mission. *Space Science Reviews*, *141*(1-4), 5–34. <https://doi.org/10.1007/s11214-008-9336-1>
- Bonnell, J. W., Mozer, F. S., Delory, G. T., Hull, A. J., Ergun, R. E., Cully, C. M., et al. (2008). The electric field instrument (EFI) for THEMIS. *Space Science Reviews*, *141*(1-4), 303–341. <https://doi.org/10.1007/s11214-008-9469-2>
- Bortnik, J., Cutler, J. W., Dunson, C., & Bleier, T. E. (2007). An automatic wave detection algorithm applied to Pc1 pulsations. *Journal of Geophysical Research*, *112*, A04204. <https://doi.org/10.1029/2006JA011900>
- Burtis, W. J., & Helliwell, R. A. (1969). Banded chorus a new type of VLF radiation observed in the magnetosphere by OGO 1 and OGO 3. *Journal of Geophysical Research*, *74*(11), 3002–3010. <https://doi.org/10.1029/JA074i011p03002>
- Fu, X., Cowee, M. M., Friedel, R. H., Funsten, H. O., Gary, S. P., Hospodarsky, G. B., et al. (2014). Whistler anisotropy instabilities as the source of banded chorus: Van Allen probes observations and particle-in-cell simulations. *Journal of Geophysical Research: Space Physics*, *119*, 8288–8298. <https://doi.org/10.1002/2014JA020364>
- Fu, X., Guo, Z., Dong, C., & Gary, S. P. (2015). Nonlinear subcyclotron resonances as a formation mechanism for gaps in banded chorus. *Geophysical Research Letters*, *42*, 3150–3159. <https://doi.org/10.1002/2015GL064182>
- Gao, X. L., Ke, Y. G., Lu, Q. M., Chen, L. J., & Wang, S. (2017). Generation of multiband chorus in the Earth's magnetosphere: 1-D PIC simulation. *Geophysical Research Letters*, *44*, 618–624. <https://doi.org/10.1002/2016GL072251>
- Gao, X. L., Lu, Q. M., Bortnik, J., Li, W., Chen, L. J., & Wang, S. (2016). Generation of multiband chorus by lower band cascade in the Earth's magnetosphere. *Geophysical Research Letters*, *43*, 2343–2350. <https://doi.org/10.1002/2016GL068313>
- Gao, X. L., Lu, Q. M., & Wang, S. (2018). Statistical results of multiband chorus by using THEMIS waveform data. *Journal of Geophysical Research: Space Physics*, *123*, 5506–5515. <https://doi.org/10.1029/2018JA025393>
- Gao, X. L., Lu, Q. M., Wang, S. J., & Wang, S. (2018). Theoretical analysis on lower band cascade as a mechanism for multiband chorus in the Earth's magnetosphere. *AIP Advances*, *8*(5), 055003. <https://doi.org/10.1063/1.5025507>
- Habagishi, T., Yagitani, S., & Omura, Y. (2014). Nonlinear damping of chorus emissions at local half cyclotron frequencies observed by Geotail at  $L > 9$ . *Journal of Geophysical Research: Space Physics*, *119*, 4475–4483. <https://doi.org/10.1002/2013JA019696>
- Hsieh, Y.-K., & Omura, Y. (2018). Nonlinear damping of oblique whistler mode waves via Landau resonance. *Journal of Geophysical Research: Space Physics*, *123*, 7462–7472. <https://doi.org/10.1029/2018JA025848>
- Li, W., Thorne, R. M., Bortnik, J., Tao, X., & Angelopoulos, V. (2012). Characteristics of hiss-like and discrete whistler-mode emissions. *Geophysical Research Letters*, *39*, L18106. <https://doi.org/10.1029/2012GL053206>
- Meredith, N. P., Horne, R. B., & Anderson, R. R. (2001). Substorm dependence of chorus amplitudes: Implications for the acceleration of electrons to relativistic energies. *Journal of Geophysical Research*, *106*(A7), 13,165–13,178. <https://doi.org/10.1029/2000JA900156>
- Ni, B. B., Thorne, R. M., Shprits, Y. Y., Orlova, K. G., & Meredith, N. P. (2011). Chorus-driven resonant scattering of diffuse auroral electrons in nondipolar magnetic fields. *Journal of Geophysical Research*, *116*, A06225. <https://doi.org/10.1029/2011JA016453>
- Omura, Y., Hikishima, M., Katoh, Y., Summers, D., & Yagitani, S. (2009). Nonlinear mechanisms of lower-band and upper-band VLF chorus emissions in the magnetosphere. *Journal of Geophysical Research*, *114*, A07217. <https://doi.org/10.1029/2009JA014206>
- Reeves, G. D., Spence, H. E., Henderson, M. G., Morley, S. K., Friedel, R. H. W., Funsten, H. O., et al. (2013). Electron acceleration in the heart of the Van Allen radiation belts. *Science*, *341*(6149), 991–994. <https://doi.org/10.1126/science.1237743>
- Roux, A., Le Contel, O., Coillot, C., Bouabdellah, A., de la Porte, B., Alison, D., et al. (2008). The search coil magnetometer for THEMIS. *Space Science Reviews*, *141*(1-4), 265–275. <https://doi.org/10.1007/s11214-008-9455-8>
- Thorne, R. M., Li, W., Ni, B., Ma, Q., Bortnik, J., Chen, L., et al. (2013). Rapid local acceleration of relativistic radiation-belt electrons by magnetospheric chorus. *Nature*, *504*(7480), 411–414. <https://doi.org/10.1038/nature12889>
- Thorne, R. M., Ni, B., Tao, X., Horne, R. B., & Meredith, N. P. (2010). Scattering by chorus waves as the dominant cause of diffuse auroral precipitation. *Nature*, *467*(7318), 943–946. <https://doi.org/10.1038/nature09467>
- Tsurutani, B. T., & Smith, E. J. (1974). Postmidnight chorus: A substorm phenomenon. *Journal of Geophysical Research*, *79*(1), 118–127. <https://doi.org/10.1029/JA079i001p00118>
- Xiao, F., Yang, C., He, Z., Su, Z., Zhou, Q., He, Y., et al. (2014). Chorus acceleration of radiation belt relativistic electrons during March 2013 geomagnetic storm. *Journal of Geophysical Research: Space Physics*, *119*, 3325–3332. <https://doi.org/10.1002/2014JA019822>
- Yagitani, S., Habagishi, T., & Omura, Y. (2014). Geotail observation of upper band and lower band chorus elements in the outer magnetosphere. *Journal of Geophysical Research: Space Physics*, *119*, 4694–4705. <https://doi.org/10.1002/2013JA019678>